Ch 283

ACTA POLYTECHNICA SCANDINAVICA

CHEMICAL TECHNOLOGY SERIES No. 283

Calculation of Multicomponent Mass Transfer between Dispersed and Continuous Phases

VILLE ALOPAEUS

Helsinki University of Technology
Department of Chemical Technology
Laboratory of Chemical Engineering and Plant Design
P.O. Box 6100
FIN-02015 HUT, Finland

Dissertation for the Degree of Doctor of Technology to be presented with due permission for public examination and debate in Auditorium Komppa at Helsinki University of Technology (Espoo, Finland) on the 15th of June, 2001, at 12 o'clock noon.

ESPOO 2001

Alopaeus, V. J., Calculation of Multicomponent Mass Transfer between Dispersed and Continuous Phases. Acta Polytechnica Scandinavica, Chemical Technology Series No. 283, Espoo 2001, 35 pp. Published by the Finnish Academies of Technology. ISBN 951-666-574-8, ISSN 1239-0518.

Keywords: Multicomponent mass transfer, Maxwell-Stefan theory, matrix approximations, mass transfer models, Population balances, liquid-liquid dispersions, stirred tank inhomogeneity, simulation

ABSTRACT

In many industrially important unit operations, mass transfer between dispersed and continuous phases takes place. The accurate and fast solution of the mass transfer model equations is essential in order to design these unit operations accurately.

The mass transfer rate between phases is calculated in two parts. The first part is to solve the interphasial mass transfer fluxes. With multicomponent systems, this is best done with the Maxwell-Stefan diffusion model along with a mass transfer model. The other part is to calculate the mass transfer area between the phases. This can be done with population balance models, preferably with a flow model that discriminates various regions of the modeled system. The flow model is needed if the phenomena affecting the development of the mass transfer area are not homogeneous in separate parts of the considered region. The mass transfer rate needed in the material balances is then a product of the mass transfer fluxes and the mass transfer area.

The mass transfer calculations with the Maxwell-Stefan model leads to complicated matrix function calculations. This is very time consuming because these models need to be solved many times during the solution of a unit operation or reactor model. Two simplifications to these complicated functions are presented in this work. The first is a method to calculate general matrix functions related to the multicomponent mass transfer models approximately. It is based on the fact that the diffusion coefficient matrices have larger diagonal than off-diagonal elements. The other approximation is a linearization of the high flux correction. The applicability of these two approximations, along with other modeling aspects, is considered with a distillation tray model. An approximation was also presented in this work for calculating diffusion, and further the mass transfer coefficients, within spherical particles.

A population balance approach is used with a stirred tank flow model to calculate drop size distributions in liquid-liquid dispersions. In order to test the applicability of the flow model with population balances, drop size distributions are measured and the drop breakage and coalescence function parameter values are estimated. The inhomogeneous character of the dispersion in a stirred tank can be used in the parameter estimation process.

PREFACE

This work was carried out at the Helsinki University of Technology in the Laboratory of Chemical Engineering and Plant Design during the years 1996–1999 and at Neste Engineering Oy at 2000.

I want to thank my advisors, Prof. Juhani Aittamaa, Prof. Harry V. Nordén, and Prof. Juha Kallas. I am also grateful to my co-authors Dr. Kari I. Keskinen and Dr. Jukka Koskinen for their assistance. I thank also all the people at the Laboratory of Chemical Engineering and Plant Design for creating academic atmosphere that helped me to accomplish this work, and all my friends for constantly asking me when my thesis will be completed.

Financial support from Neste Oy Foundation is gratefully acknowledged.

I am grateful to Heli for understanding and encouragement during this work.

Helsinki, 06. 12. 2000

Ville Alopaeus

CONTENTS

LIST OF PUBLICATIONS 5
LIST OF SYMBOLS 6
1 INTRODUCTION 8
2 INTERPHASIAL MASS TRANSFER AND THE MATERIAL BALANCES 9
2.1 Mass transfer fluxes 9
2.2 Material balances 12
3 CALCULATION OF MULTICOMPONENT MASS TRANSFER FLUXES 14
3.1 Mass transfer coefficients 14
3.2 High flux correction 17
3.3 Some approximations to multicomponent mass transfer calculations 17
3.4 Solution of the interfacial mass transfer flux models 20
4 CALCULATION OF MASS TRANSFER AREA 22
4.1 Population balances 22
4.2 Flow model 24
4.3 Drop breakage and coalescence function parameter estimation 25
4.4 Drop size distribution measurements 25
4.5 Functions related to drop breakage and coalescence 26
4.6 Results from the single block model 28
4.7 Results from the multiblock model 29
5 CONCLUSIONS 32
REFERENCES 33

LIST OF PUBLICATIONS

This thesis is based on the following publications

1. Alopaeus, V., Aittamaa, J., Nordén, H. V., Approximate High Flux Corrections for Multicomponent Mass Transfer Models and Some Explicit Methods, *Chem. Eng. Sci.* Vol. 54 (1999) pp. 4267-4271.
2. Alopaeus, V., Nordén, H. V., A Calculation Method for Multicomponent Mass Transfer Coefficient Correlations, *Computers & Chem. Eng.* Vol. 23 (1999), pp. 1177-1182.
3. Alopaeus, V., Koskinen, J., Keskinen, K. I., Simulation of the Population Balances for Liquid-Liquid Systems in a Nonideal Stirred Tank, Part 1 Description and Qualitative Validation of the Model, *Chem. Eng. Sci.* Vol. 54 (1999), pp. 5887-5899.
4. Alopaeus, V., Aittamaa, J., Appropriate simplifications in calculation of mass transfer in a multicomponent rate-based distillation tray model, *Ind. Eng. Chem. Res.* Vol. 39 (2000), pp. 4336-4345.
5. Alopaeus, V., Mass Transfer Calculation Methods for Transient Diffusion Within Particles, *AIChE J.* **46** (2000) pp. 2369-2372.
6. Alopaeus, V., Keskinen, K. I., Koskinen, J., Utilization of Population Balances in Simulation of Liquid-Liquid Systems in Mixed Tanks, Presentation at AIChE Annual meeting 2000, Los Angeles, USA

THE AUTHOR'S CONTRIBUTION

The author prepared all papers and calculated all results. The scientific content and calculation methods in all the papers were developed by the author, except for paper 2, in which the method was developed by the author in co-operation with Prof. Harry V. Nordén.

LIST OF SYMBOLS

$\#(V_i)$	index number of drop class of characteristic volume V_i	( )
Δa	width of droplet class	(m)
[A]	a matrix appearing in the Maxwell-Stefan models	( )
[B]	matrix of inverted binary diffusion coefficients	(sm^{-2})
[D]	matrix of diffusion coefficients	(m^2s^{-1})
[I]	identity matrix	( )
[k]	mass transfer coefficient matrix	(ms^{-1})
$A(a)$	population density based on diameter	(m^{-1})
a	parameter	( )
a	linearization parameter	( )
a	drop diameter	(m)
a_{32}	Sauter mean diameter, $a_{32} = \Sigma\, a_i^3 / \Sigma\, a_i^2$	(m)
b	parameter	( )
c	concentration	($mol \cdot m^{-3}$)
$C_1 ... C_5$	empirical constants	
c_t	total concentration	($mol \cdot m^{-3}$)
D_i	impeller diameter	(m)
$\mathbb{D}_{ij}$	binary diffusion coefficients	(m^2s^{-1})
$F(a_i, a_j)$	binary coalescence rate between droplets a_i and a_j in unit volume	(m^3s^{-1})
[Fo]	matrix of Fourier numbers	( )
$g(a)$	breakage frequency of drop size a	(s^{-1})
$h(a_i, a_j)$	collision frequency between droplets a_i and a_j in unit volume	(m^3s^{-1})
J	diffusion flux	($mol \cdot m^{-2}s^{-1}$)
l	film thickness	(m)
m	parameter	( )
N	mass transfer flux	($mol \cdot m^{-2}s^{-1}$)
n	number density	(m^{-3})
n	number of components	( )
nc	number of drop size categories	( )
N_P	impeller power number	( )
N_t	total flux	($mol \cdot m^{-2}s^{-1}$)
r	reaction rate (production of a component)	($mol \cdot m^{-3}s^{-1}$)
t	time	(s)
V	molar flow	($mol \cdot s^{-1}$)
x, x_B, x_I	mole fraction, mole fraction in bulk, mole fraction at interface	( )
Y_i	number concentration of drop class i	(m^{-3})
$Y_{i,in}$, $Y_{i,out}$	flow of drop class i per unit volume into and out from the region of interest, respectively	($s^{-1}m^{-3}$)

Greek symbols

ε	turbulent energy dissipation (per unit mass)	(m^2s^{-3})
σ	interfacial tension	(Nm^{-1})
ϕ	volume fraction of dispersed phase	( )
$[\Xi]$	high flux correction matrix	( )
$[\Psi]$	mass transfer rate factor matrix	( )
$\nu(a)$	number of drops formed when drop of size a is broken	( )
$\beta(a_i, a_j)$	probability that a drop of size a_i is formed when a drop of size a_j breaks	(m^{-1})
$\lambda(a_i, a_j)$	collision efficiency between drops a_i and a_j	( )
Ψ_{ave}	scalar average mass transfer rate factor	( )
μ_D, μ_C	dispersed phase and continuous phase viscosities	(Pas)
ρ_D, ρ_C	dispersed phase and continuous phase densities	(kgm^{-3})

Mathematical notations

( )	column matrix	various
[ ]	square matrix	various

1 INTRODUCTION

Mass transfer occurs between immiscible phases if the phases are not in equilibrium, i.e. if the chemical potentials of the two phases are different. This deviation from equilibrium is the driving force for mass transfer between the phases.

Most unit operations in chemical engineering include exchange of material between phases. In distillation, extraction and absorption, among others, the mass transfer between phases is exactly the desired operation. Usually the desired mass transfer is achieved by using either mechanical or thermal energy. Sometimes a mass separating agent can be used. In these cases, some components are deliberately added to the system in order to carry out the desired separation. For example, in extraction a solvent is used to separate components whose miscibility to the solvent varies. Mechanical energy is brought to the mass transfer process by e.g. stirring the multiphase suspension to increase the area between the phases. Thermal energy is used in e.g. distillation, where the desired vapor and liquid flows through a distillation column are obtained by boiling the liquid and condensing the vapor. Calculation of mass transfer is then essential in understanding and designing these unit operations.

In multiphase reactors, interphasial mass transfer may limit the observed reaction rate. The two phases may be present because some of the reactants are immiscible or because the reactions are carried out with solid catalyst. Presence of two phases is utilized also in so-called reactive separation processes, where reaction and separation occurs simultaneously. There are some advantages in these kinds of processes; for example, the reaction equilibrium limitations can be avoided by transferring the product out from the reaction phase. This results in a faster observed overall reaction rate.

Mass transfer limitations are rarely desired in reactors, so mechanical energy needs to be brought to the reaction mixture to enhance mass transfer. On the other hand, excess energy consumption is not wanted either. In these cases, accurate mass transfer calculations are needed to design the reactors properly.

2 INTERPHASIAL MASS TRANSFER AND THE MATERIAL BALANCES

Unit operations and reactors are usually modeled by a set of algebraic or differential equations, or by a combination of these. These models consist of equations for material balances for each component, energy balances, phase equilibrium and other thermodynamic equations, reaction rate equations for reactive systems, pressure drop equations, and other system specific equations.

Interphase mass transfer appears in these models in the material balance equations. The mass transfer rate is usually a product of two terms: the mass transfer fluxes (the amount of components changing phase in unit time per unit interface area) for each component, and the mass transfer area.

In order to calculate interphase mass transfer, material balances need to be formulated for the phases between which mass is transferred.

2.1 Mass transfer fluxes

The material balance for a differential volume element fixed in space (or in phase boundary if mass transfer between phases is considered) is

$$\frac{\partial c_i}{\partial t} + \nabla \cdot N_i = r_i \tag{1}$$

The mass transfer fluxes, N_i, are made up of diffusive and convective terms

$$N_i = J_i + x_i N_t \tag{2}$$

Several methods are presented for calculating diffusive fluxes. These methods can usually be written in a form of a (generalized) Fick's law

$$J_i = -c_t \sum_{k=1}^{n-1} D_{ik} \nabla x_i \tag{3}$$

where diffusion of component i is affected by all independent mole fraction gradients.

The most fundamental method so far for calculating D_{ik}'s seems to be the Maxwell-Stefan equation, which is based on conservation of momentum in collisions between various molecule types (various components considered). Concentration dependent D_{ik}'s are calculated from the mole fractions of the species and the binary diffusion coefficients (the $Đ_{ij}$'s) [7, 8].

Diffusion fluxes are often presented in a compact matrix form

$$(J) = -c_t[D]\nabla(x) \tag{4}$$

Here (J) is a column matrix of the diffusion fluxes $J_1...J_{n-1}$. [D] is a n-1 square matrix of diffusion coefficients. (x) is a column matrix of the mole fractions.

According to the Maxwell-Stefan diffusion model, the following elements for the [D] matrix are obtained. First a matrix of inverted binary diffusion coefficients is calculated

$$\begin{aligned} B_{ii} &= \frac{x_i}{Đ_{in}} + \sum_{\substack{k=1 \\ k\neq i}}^{n} \frac{x_k}{Đ_{ik}} \\ B_{ij} &= -x_i\left(\frac{1}{Đ_{ij}} - \frac{1}{Đ_{in}}\right) \end{aligned} \tag{5}$$

[D] is then the inverse of [B]

$$[D] = [B]^{-1} \tag{6}$$

Together with the total flux induced convective mass transfer term, the mass transfer flux equation becomes

$$(N) = -c_t[D]\nabla(x) + N_t(x) \tag{7}$$

This could be inserted into the material balance equation (1), resulting in the following equation:

$$\frac{\partial(c)}{\partial t} = \nabla \cdot \left(c_t [D] \nabla(x)\right) - \nabla \cdot \left(N_t(x)\right) + (r) \qquad (8)$$

where (c) is a column matrix of component concentrations [8].

This equation, together with differential energy and momentum balance equations and equations of state (and often separate phase equilibrium equations), describes the system to be analyzed. Mass transfer between phases (the mass transfer fluxes) is calculated by a suitable integrated mass transfer model. Geometric models for the phase boundary (e.g. the film model, the penetration model) are needed for initial and boundary values for differential equation (7) or (8). In non-stationary cases the composition gradients are calculated from equation (8) and then used for the mass transfer flux calculations. Some approximations must usually be made so that the equations can be integrated, preferably analytically. Usually, the total concentration and the matrix of diffusion coefficients are assumed constant along the diffusion path. Also, non-diffusional interactions are often neglected.

If the system is thermodynamically highly nonideal, the deviation from ideal behavior can be taken into account with a separate thermodynamic nonideality correction matrix. The thermodynamic nonideality matrix takes into account the fact that the actual driving forces for diffusion are not the mole fraction gradients, but the gradients of chemical potentials [8].

For a general analytical solution, the reaction term of equation (8) must be assumed negligible compared to the diffusion term. These assumptions are valid for non-reacting systems, or when the reactions are not very fast. A fast reaction is defined loosely here so that it affects noticeably concentration profiles close to phase boundary. In these cases, the reaction-diffusion equation (8) must usually be solved numerically. Other than fast reactions affect mass transfer only by changing bulk compositions. This assumption is made here.

Diffusion equation (8) can be linearized by assuming that the matrix [D] and the scalar c_t are not mole fraction dependent in the mass transfer region. This manner of proceeding is referred as the linearized theory of mass transfer, or Toor, Stewart and Prober approach [9, 10]. Although some analytical solutions to the mass transfer models with the exact Maxwell-Stefan approach are available (Krishna & Standart, 1976), the linearization approach is taken here. The validity of the linearization is considered by Smith and Taylor [11] and by Young and Stewart [12].

If the reaction effects to mass transfer are assumed negligible, and the linearized mass transfer approach is taken, eq. (8) can be written as

$$c_t \frac{\partial(x)}{\partial t} = c_t[D]\nabla^2(x) - \nabla\left(N_t(x)\right) \tag{9}$$

Integration of this differential material balance equation or the flux equation (7) can be completed once a geometric model for the phase boundary has been defined. The integrated mass transfer equation is then used in the total (integrated) material balance equations of the whole system, e.g. in reactor or mass transfer device models. The mass transfer models considered here are formed for one spatial variable.

2.2 Material balances

The amount of material exchanged between phases needs to be calculated for the material balance of unit operation or multiphase reactor models. The amount of material exchanged in unit time is a product of the mass transfer fluxes and the interfacial area.

$$V = NA \tag{10}$$

where N is the mass transfer flux, i.e. moles transferred in unit time divided by the mass transfer area, and A is the total mass transfer area between the phases.

If segregation of the dispersed phase is significant, an additional variable describing the segregated property is needed. By segregation, it is meant that some property of the

dispersed phase is not homogeneous or constant throughout the system, so that the dispersed phase cannot be assumed completely mixed. Usually this property is the particle (solid or fluid) size; i.e. particles of various sizes behave differently. In addition, residence time of particles in a balance region may be the segregating variable. In case of segregation, the dispersed phase must be divided into discrete categories, and mass transfer needs to be calculated separately for each category. The material balances must then be formulated separately for each category.

3 CALCULATION OF MULTICOMPONENT MASS TRANSFER FLUXES

A geometric model for the phase boundary needs to be defined in order to calculate the mass transfer fluxes. Two models have generally been used; namely, the film model and the penetration model. In the film model, mass transfer is assumed to occur in a film next to the interface, and in this film, the turbulent diffusion is assumed negligible. Beyond this film, referred usually as a bulk phase, the molecular diffusion is assumed negligible compared to the turbulent diffusion. This results in constant concentrations in the bulk.

In the penetration model, a volume of bulk fluid is assumed to be exposed to the interface, and diffusion is assumed to take place for a certain contact time. After that, the volume returns to the bulk phase, where concentrations are assumed constant.

The following equation can be derived for multicomponent mass transfer calculations [8]. It applies both to the film and the penetration models. Here it is written in a form where thermodynamic nonidealities are neglected. A correction matrix for thermodynamic nonidealities needs to be included, if the deviation from ideal behavior is considered important [8].

$$(N) = c_t[k][\Xi](x_B - x_I) + (x_B)N_t \tag{11}$$

Here [k] is the matrix of mass transfer coefficients and [Ξ] is the matrix of high flux corrections. These matrices are calculated slightly differently for the film and the penetration models.

3.1 Mass transfer coefficients

For the film theory, the matrix of mass transfer coefficient is defined as

$$[k] = [D] / l \tag{12}$$

where l is the film thickness. For the penetration theory, the mass transfer coefficients are also functions of the diffusion coefficients (usually to a power of 0.5), and the chosen contact time distribution for the volume elements. However, the film thickness or the contact time distribution is rarely known. Then empirical correlations for the mass transfer coefficients must be used. These are often of the following form

$$[k] = a\cdot[D] + b\cdot[D]^m \tag{13}$$

Here the dependence of the mass transfer coefficients on the diffusion coefficients is emphasized due to the matrix nature of the multicomponent mass transfer coefficient correlations. Generally, parameters a and b depend on physical properties. This equation reduces to a theoretical film model by setting $a = 1/l$ and $b = 0$, and to a penetration model by setting $m = 0.5$ and $a = 0$. In the latter case, the factor b depends on the chosen contact time distribution.

For the dispersed phase side, an analytical solution to the diffusion equation can be derived. This requires that some assumptions are fulfilled. If the dispersed phase consists of stagnant spherical particles (solid or fluid), and the interfacial compositions are not time dependent, the following solution can be found for the transient diffusion equation

$$[k][D]^{-1} / a = \frac{2\pi^2}{3}\left(\sum_{n=1}^{\infty}\exp\left(-n^2\pi^2[Fo]\right)\right)\left(\sum_{n=1}^{\infty}\frac{1}{n^2}\exp\left(-n^2\pi^2[Fo]\right)\right)^{-1} \tag{14}$$

where [Fo] is the matrix of Fourier numbers, defined as $[Fo] = 4t/a^2[D]$. For the case of adsorption to solid adsorbent, the Fourier number needs to be modified to take into account the adsorption equilibrium. The equation (14) is an infinite series of matrix functions, and especially for short contact times, many terms are needed in order to converge the series. A rational approximation to this equation can be used to help the solution. The following rational function follows the exact solution closely [5].

$$[k][D]^{-1}/a = \frac{a_0}{\sqrt{\pi}}[Fo]^{-1/2} + \left(a_1 \cdot [Fo]^{0.5} + a_2 \cdot [Fo] + \frac{2\pi^2}{3} a_5 \cdot [Fo]^{1.5}\right) \cdot \left([I] + a_3 \cdot [Fo]^{0.5} + a_4 \cdot [Fo] + a_5 \cdot [Fo]^{1.5}\right)^{-1} \quad (15)$$

This is based on asymptotic solutions for both short and long contact times. The intermediate contact time region is described by a rational function, where five parameters are estimated to represent the exact solution. The following parameters can be used to calculate the instantaneous mass transfer coefficients: $a_0 = 2$, $a_1 = 117346$, $a_2 = 39596$, $a_3 = 62166$, $a_4 = 31169$, and $a_5 = 337258$. If time averaged values are needed, the same function applies, but with the following parameters: $a_0 = 4$, $a_1 = 63237$, $a_2 = 71892$, $a_3 = 33616$, $a_4 = 45628$, and $a_5 = 116673$. The first set of parameters can be used when the unit operation model is solved with respect to time, and the second when average mass transfer rates over a time period are needed in an unit operation model [5].

In Figure 1, the exact series expansion solution to the instantaneous case is shown with the rational approximation. As can be seen, the two solutions are almost indistinguishable.

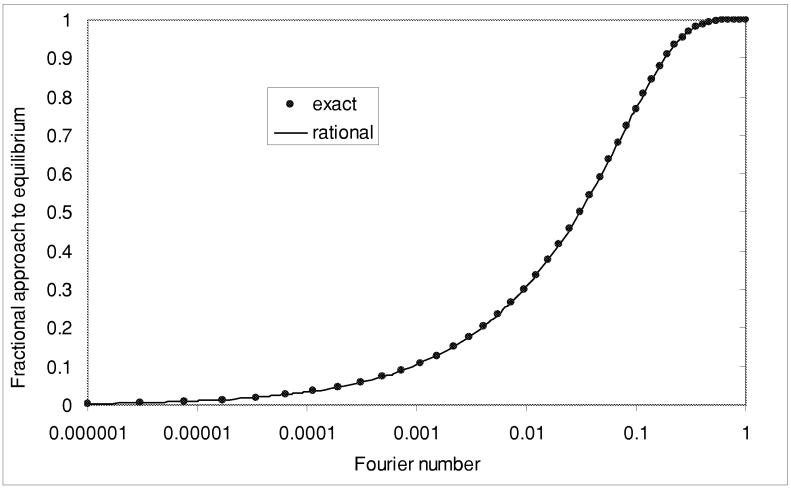

Figure 1. Exact solution to diffusion in a sphere and a rational approximation

3.2 High flux correction

The matrix of high flux corrections takes into account the fact that the mole fraction gradients are not linear in the diffusion region if the convective mass transfer is noticeable. This can be seen from the mass transfer flux equation (7). Since the mass transfer fluxes are constant along the diffusion path, and the mole fractions vary, then the diffusive fluxes must vary as well. But as the diffusion coefficients were also assumed constant, then as a result, the mole fraction gradients must be curved. The matrix of high flux corrections accounts for this curvature. For the film theory, the following matrix function can be derived to take the high flux correction into account [8].

$$[\Xi] = [\Psi][\exp[\Psi] - [I]]^{-1} \tag{16}$$

For the penetration theory it is

$$[\Xi] = \exp\left(-[\Psi]^2/\pi\right)\left([I] + \operatorname{erf}\left([\Psi]/\sqrt{\pi}\right)\right)^{-1} \tag{17}$$

In these equations, $[\Psi]$ is the matrix of mass transfer rate factors. For the linearized mass transfer theory, the changes in the total concentration and in the diffusion coefficient matrix are neglected in the region where the mass transfer is calculated, and averages are used. Then the mass transfer rate factor matrix is

$$[\Psi] = N_t \cdot \ell / c_t \, [D_{av}]^{-1} = N_t / c_t \, [k_{av}]^{-1} \tag{18}$$

The subscript $_{av}$ in the mass transfer coefficient matrix notes that the matrix is calculated at the average compositions in the mass transfer region [1, 8].

3.3 Some approximations to multicomponent mass transfer calculations

Usually complicated matrix functions are needed to calculate the multicomponent mass transfer fluxes with the Maxwell-Stefan models. This is very time consuming, especially since the mass transfer models are usually a part of a more complicated

model for a mass transfer unit operation or a reactor. Often these unit operation models are combined into a flowsheet of several unit operations and reactors [13]. The solution of the whole flowsheet may then need sequential iterative solutions, and the number of mass transfer flux iterations may become very large. Reasonable approximations are welcomed to describe the fluxes accurately but with a lower computational burden. The following approximations help to calculate the matrix functions with considerably less work than the exact formulations.

Krishna and Standart [14] suggested that the mass transfer coefficient correlations may be used directly to the binary diffusion coefficients, and then the matrix of multicomponent mass transfer coefficients could be calculated from the binary mass transfer coefficients. This is based on the film theory, and if a single well-defined film thickness for all components can be used, this method reduces to the definition of mass transfer coefficients in the film model. In that case, however, no matrix function calculations are needed in the mass transfer coefficient correlations.

The matrix fractional powers rising from the multicomponent diffusion models can be calculated approximately, after noting that the diffusion coefficient matrices must have large diagonal elements compared to the off-diagonal. The reason for this is that for a thermodynamically stable phase, the diffusion coefficient matrix must be positive definite [8, 15]

For the problem $[A] = [D]^p$, we can then use the following approximate formulas [2]

$$A_{ii} = D_{ii}^p \qquad \text{for diagonal elements, and} \qquad (19)$$

$$A_{ij} = D_{ij}\frac{D_{ii}^p - D_{jj}^p}{D_{ii} - D_{jj}} \qquad \text{for off-diagonal elements.} \qquad (20)$$

Other matrix functions can be approximated similarly. For a general problem $[A] = f([D])$ we can use the following

$$A_{ii} = f(D_{ii}) \qquad \text{for diagonal elements, and} \qquad (21)$$

$$A_{ij} = D_{ij}\frac{f(D_{ii}) - f(D_{jj})}{D_{ii} - D_{jj}} \qquad \text{for off-diagonal elements.} \qquad (22)$$

When this method is applied to the multicomponent mass transfer coefficient correlations, generally very accurate results are obtained. In numerical simulations, for four component systems the errors are usually within 1 %. For a larger number of components the errors increase, but are usually within 10 % in all the calculated cases. These errors were calculated by comparing the approximate results to the pure multicomponent approach where the diffusion coefficient matrices are used in all places instead of the scalar single component diffusion coefficients. The errors were comparable to the errors in the binary mass transfer coefficient method, but usually slightly lower [2].

Other approximation can be made by linearizing the high flux correction. This leads to the following approximate high flux correction [1]

$$[k][\Xi] = [k] - a \cdot N_t/c_t[I] \qquad (23)$$

where the linearization parameter a can be calculated from the following equations. For the film theory

$$a = \frac{1}{\Psi_{ave}} - \frac{1}{\exp(\Psi_{ave}) - 1} \qquad (24)$$

and for the penetration theory

$$a = \frac{1}{\Psi_{ave}}\left(1 - \frac{\exp\left(\Psi_{ave}^2/\pi\right)}{\left(1 + \mathrm{erf}\left(\Psi_{ave}/\sqrt{\pi}\right)\right)}\right) \qquad (25)$$

Here

$$\Psi_{ave} = N_t \cdot (n - 1) / (c_t \cdot \Sigma k_{ii}) \quad (26)$$

In practical calculations, the approximation error that results when using this method is negligible even when the total flux is significant. Therefore, the linearized high flux correction can be used in all cases with confidence. In numerical simulations of a rate-based distillation tray model, which is one of the most typical mass transfer situations, the errors rising from the approximate calculations of the high flux correction or the mass transfer coefficient matrix were negligible compared to the effect of other modeling assumptions [1, 4].

3.4 Solution of the interfacial mass transfer flux models

In the calculation of the interfacial fluxes, iterative solution is needed. At minimum, the iterated variables are the interface compositions, temperature, the distribution coefficients, and the total flux. In these models, the mass and heat transfer fluxes across the interface must be equal on both sides of the interface. Simultaneously the phase equilibrium at the interface needs to be fulfilled. The remaining two equations are the obvious (but sometimes forgotten) summation relations, since the mole fractions must sum up to unity on both sides of the interface [4].

If mass transfer between bulk fluid and a solid catalyst is calculated, the phase equilibrium needs not to be calculated (unless an adsorption equilibrium model is used). Then the iterated variables are the compositions at the surface, temperature the and total flux.

If complete matrix calculations are performed, the matrix multiplications should be carried out from right to left, so that no multiplications with two square matrices need to be done [16]. Then the most time consuming matrix function calculations are the matrix function evaluations at the high flux correction, the matrix fractional power calculations at the mass transfer coefficient correlations, and the matrix inversions both in the high flux corrections and in the nonlinear algebraic equation solver.

When the unit operation model consists of nonlinear algebraic equations, mass transfer is preferably calculated simultaneously with the other model equations. If the unit

operation consists of differential equations, mass transfer needs to be calculated many times during the integration of the unit operation model. Then it is essential to use good initial values for the iterated variables. Good initial values can be obtained from the previous iterative solution, which is spatially or with respect to time close to the present location. Then the mass transfer flux calculations usually converge very rapidly.

4 CALCULATION OF MASS TRANSFER AREA

To model a mass transfer situation, the mass transfer area needs to be known. In case of mass transfer between dispersed and continuous phases, this is the surface area of the dispersed phase. Generally, the surface area may depend on the physical properties of the system, the energy input on the system, and the volume fraction of the dispersed phase.

New surface forms when the energy put into the system is dissipated to surface energy. As an example, in gas-liquid or liquid-liquid dispersions bubbles or droplets are broken when the dispersion is stirred. In many classical unit operations, such as distillation, the energy to form surface area is brought by letting one of the phases to flow through orifices, and the pressure drop is partly transformed into surface energy.

Classically, empirical or semi-empirical correlations have been used to calculate the surface area in various dispersed phase systems. These correlations are formed e.g. by equating the total energy dissipation to the system, and the surface energy terms. Adjustable variables are then used to fit these correlations to experimental data. A common feature for these correlations is that they are simple to use, but they are limited in applicability. In most cases, they apply only for the systems with similar physical properties and dimensions for which they are developed.

4.1 Population balances

A more detailed description of the dispersed phase surface area can be obtained by using the population balance models. Then separate models can be used to describe all the phenomena affecting surface area. Mechanistic models can be formulated for bubble or drop breakage and coalescence, formation of new bubbles or drops, convection into or out from the considered balance region, growth or shrinkage due to mass transfer, and other possible effects, such as occurrence of reactions that do not conserve volume. In the following development, the dispersed phase is referred as the drop phase, although the development can be used straightforwardly for other continuous – dispersed phase systems, such as gas in liquid, solid in liquid etc. A

stirred tank is used as an example of a process to be modeled, but the population balance approach is also applicable to any other multiphase system.

For a chemically equilibrated liquid-liquid dispersion (no growth or shrinkage of droplets due to mass transfer or reaction), the population balance equation for a unit volume is

$$\frac{d(nA(a))}{dt} = n_{in}A(a) + \int_{a}^{\infty} \nu(a')\beta(a,a')g(a')nA(a')da'$$
$$+ \int_{0}^{a/\sqrt[3]{2}} \lambda\left((a^3 - a'^3)^{1/3}, a'\right)h\left((a^3 - a'^3)^{1/3}, a'\right)nA\left((a^3 - a'^3)^{1/3}\right)nA(a')da' \qquad (27)$$
$$-n_{out}A(a) - g(a)nA(a) - nA(a)\int_{0}^{\infty} \lambda(a,a')h(a,a')nA(a')da'$$

Here the term on the left side is the time rate of change of the population density function. The terms on the right side are: flow of drops into the balance region, birth of drops by breakage, birth of drops by coalescence, flow of drops out from the balance region, disappearance of drops due to breakage, and disappearance of drops due to coalescence [17, 18].

This integro-differential equation can be solved by dividing the drop population density into several discrete classes, and calculating the integrals in the above equation numerically. The following working equations are then obtained for the discrete drop classes [3]

$$\frac{dY_i}{dt} = Y_{i,in} + \sum_{j=i+1}^{nc} \nu(a_j)\beta(a_i, a_j)g(a_j)Y_j\Delta a + \sum_{j=1}^{\#(V_i/2)} F\left(\left(a_i^3 - a_j^3\right)^{1/3}, a_j\right)Y_iY_j$$
$$- Y_{i,out} - g(a_i)Y_i - Y_i\sum_{j=1}^{\#(V_{nc}-V_i)} F(a_i, a_j)Y_j \qquad (28)$$

This set of ordinary differential equations can be solved with a standard initial - value ordinary differential equation solver.

4.2 Flow model

In stirred tanks, the main phenomenon affecting drop breakage and coalescence is the dissipation of turbulent energy. This dissipation varies several orders of magnitude in various regions of the tank, being greatest near the impeller where the turbulent vortices appear, and lowest far away from the impeller. Drop breakage occurs almost exclusively near the impeller, but coalescence throughout the vessel. Then the drop sizes increase as the suspension circulates at the quiescent parts of the vessel. Therefore, a flow model describing these various regions is considered to improve the results obtained with the population balance models compared to a simple model where the vessel average turbulence properties are used. In Figure 2, a compartmentalization of a stirred tank is shown.

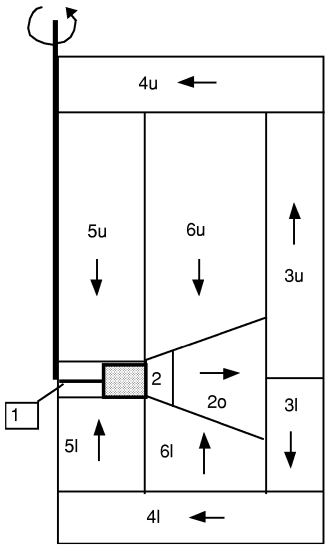

Figure 2. Multiblock model for a stirred tank

In this model, the population balances are solved in each of the regions separately. The breakage and coalescence of drops are calculated with the local turbulence properties. Furthermore, convection of drops between the regions is calculated from the known flow rates. A detailed description of the flow model is presented in [3].

4.3 Drop breakage and coalescence function parameter estimation

When a multiblock flow model is used, the parameters used in the drop breakage and coalescence functions should be estimated by using a similar flow model. The local drop size distributions are measured from a stirred tank and the drop breakage and coalescence parameters are estimated with a nonlinear parameter optimization algorithm. With only vessel averaged turbulence values, transients after an impeller speed change can be used to identify the drop breakage and coalescence rate parameters. With a multiblock model, vessel inhomogeneity can be used in addition with the transients to identify the parameters. This approach has some advantages compared to using vessel-averaged transient drop size distributions only. Longer time-averaged measurements are much more reliable than short time measurements. Other aspect favoring time-averaged local measurements is that in the population balance models, the flows are assumed to reach the new steady state immediately after the impeller speed step change. This is not quite correct, and if the transient times in the evolution of the drop size distributions are of the same order of magnitude than the transients for the flows to reach the new steady state, the use of the transient drop sizes calculated with the steady state turbulence levels are questionable [6].

4.4 Drop size distribution measurements

In order to verify the usefulness of the present model, some experiments with immiscible liquids were carried out, and the results were used to estimate the parameters of the drop breakage and coalescence rate functions [6]. The laboratory vessel was a 50-liter standard stirred tank with four baffles. The stirrer was a six-bladed Rushton turbine, with which the speed can be set without step changes. The experimental system was an Exxsol in water-dispersion, and the volume fraction of the dispersed Exxsol was 0.4 in all experiments. This volume fraction is so high that the dispersion can be considered quite dense.

Exxsol is a commercial organic solvent, with the following measured physical properties at room temperature: density 800 kg/m^3, viscosity 1.0 cP, and surface tension (against air) 24.4 mN/m. Interfacial tension between the organic solvent and water was

obtained by subtracting the surface tension of Exxsol from the surface tension of water. The interfacial tension was 43.6 mN/m.

Drop size distributions were measured using a Lasentec® FBRM (Focused Beam Reflectance Measurement) device. It is based on a rapidly rotating laser beam. The measured property of the dispersion is the drop chord length distribution. This means that the laser beam randomly measures chord lengths of passing drops, and thus a distribution of chord lengths is obtained even for droplets of uniform size. The measured distribution must then be converted into a drop size distribution by assuming spherical droplets. This procedure is described by Tadayyon and Rohani [19]. The drop size range is divided into 38 channels, and the number of drops belonging to each of these channels is measured. Typically, several hundreds or thousands of drops are measured per second.

4.5 Functions related to drop breakage and coalescence

After testing several sets of drop breakage and coalescence functions, the following functions were found to represent the experimental data with reasonable accuracy [6]. For the breakage frequency, the following function was found to give good results:

$$g(a_i) = C_1 \varepsilon^{1/3} \operatorname{erfc}\left(\sqrt{C_2 \frac{\sigma}{\rho_C \varepsilon^{2/3} a_i^{5/3}} + C_3 \frac{\mu_D}{\sqrt{\rho_C \rho_D}\, \varepsilon^{1/3} a_i^{4/3}}} \right) \tag{29}$$

This is based on a drop breakage frequency function proposed by Narsimhan, Gupta & Ramkrishna [20]. The original form was extended by including viscous forces in the energy balance for the drop breakage. Furthermore, all the parameters C_1, C_2, and C_3 were left as adjustable, and a dependency on energy dissipation to a power of 1/3 was assumed.

For the drop coalescence, the following functions are used. The drop collision term of Coalaloglou and Tavlarides [21] is used. It stands as

$$h(a_i, a_j) = C_4 \frac{\varepsilon^{1/3}}{1+\phi}(a_i + a_j)^2 \left(a_i^{2/3} + a_j^{2/3}\right)^{1/2} \tag{30}$$

A simplified form of the coalescence efficiency function of Tsouris & Tavlarides [22] is used [3]:

$$\lambda(a_i, a_j) = \left(\frac{0.26144\mu_D}{\mu_C} + 1\right)^P$$

$$P = \left(-\frac{C_5\mu_C}{\rho_C N_P{}^{1/3}\varepsilon^{1/3}(a_i + a_j)^{2/3} D_i^{2/3}}\right) \tag{31}$$

The product of $h(a_i, a_j)$ and $\lambda(a_i, a_j)$ is then the coalescence rate function $F(a_i, a_j)$.

Yet the daughter drop size function needs to be specified. It gives the distribution of the formed drops when a breakage occurs. The following function was found to give good results [23].

$$\beta(a_i, a_j) = \frac{90a_i^2}{a_j^3}\left(\frac{a_i^3}{a_j^3}\right)^2\left(1 - \frac{a_i^3}{a_j^3}\right)^2 \tag{32}$$

There are five parameters in the drop rate functions chosen for the parameter estimation. Due to limited experimental data, especially with systems with varying physical properties, all of the parameters could not be identified properly. Thus, C_3 was set to 0.2 and C_5 to 2000 at the last phase of the estimation procedure, and three parameters, namely C_1, C_2, and C_4 were left to be optimized. The frozen coefficient values were obtained by reasoning from the extrapolation studies with various physical properties, and these should not be considered to have any other but order of magnitude accuracy. It must also be noted that the parameters and the functional forms are not independent, but a consistent set of equations and corresponding parameters must be used whenever the drop size distributions are calculated.

4.6 Results from the single block model

In the single block model, three parameters were estimated along with the two that were kept constant during the estimation procedure. Three measured steady state population distributions were used, one before the step change to a higher impeller speed, one after the change, and one after the step change back to the lower value. Besides that, two transient distributions after the step change to the higher impeller speed were used. In all these cases, the Sauter mean diameter and the population densities at four locations of the distribution were used. Hence, totally 25 experimental points were used in the parameter estimation procedure [6].

The optimal parameter values for the single block model were $C_1 = 0.986$, $C_2 = 0.892 \cdot 10^{-3}$, and $C_4 = 0.433 \cdot 10^{-3}$. The estimated Sauter mean diameters were quite close to the average measured values, as can be seen from the Figure 3. Some deviation remains in the population density distribution, as shown in Figure 4.

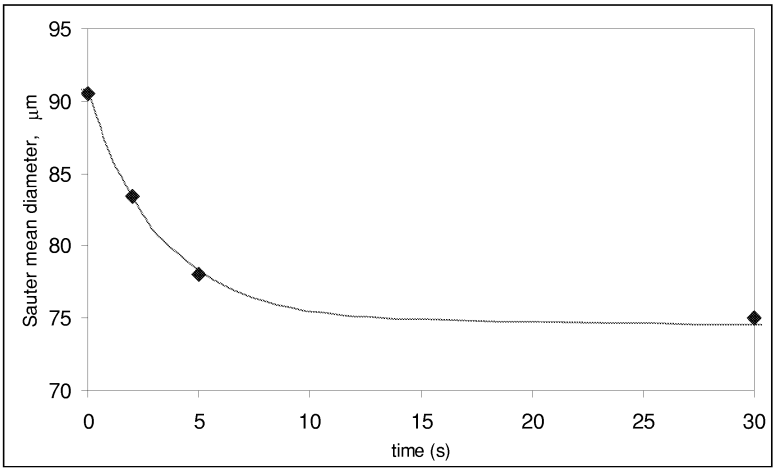

Figure 3. Simulated and measured Sauter mean diameters for the averaged vessel properties during a transient between two steady states.

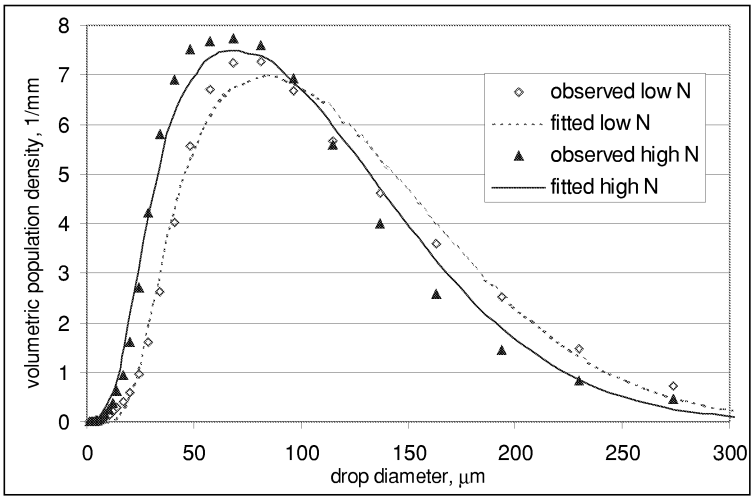

Figure 4. Simulated and measured volumetric population densities for the averaged vessel properties at steady states.

4.7 Results from the multiblock model

In the multiblock model, we have two sources of transient data for the population balance parameter estimation. The first one is to use the transient data as the impeller speed is altered, similarly to the single block model. The other source is vessel inhomogeneity from both the steady state measurements, and measurements taken during the transients. As the dispersion flows into the impeller region, the drops are broken, and during the circulation, they collide and coalesce. Then the parameters for the breakage functions can be estimated separately by measuring the drop size distributions at various points in the circulation region. The longer the time period over which the distributions are measured (time-averaged), the more accurate are the results. Thus, parameter estimation with the multiblock model and several measuring points should give more reliable parameter values than the vessel averaged model with only transients in impeller speed. Another source of error, when the transient response data is used, is that the flow fields are assumed to reach their new steady states immediately after a step change in the impeller speed. For turbulent energy dissipation, this may be a reasonable assumption, but for the flow fields, there are transients of a few seconds even for small-scale vessels. A problem with the measurements at various locations in

the vessel is that the measuring probe may slightly alter the flow fields. Of course, if the measured drop size distributions at various locations of the tank are entirely homogeneous, then the transient parameters cannot be identified by using local measurements [6].

The drop rate functions were the same than in the single block model. The optimized parameter values for the multiblock model were $C_1 = 3.68$, $C_2 = 0.775 \cdot 10^{-3}$, and $C_4 = 1.55 \cdot 10^{-3}$. In Figure 5, the measured and the estimated Sauter mean diameters from two blocks are shown. These correspond to the blocks 3l and 6u of Figure 2.

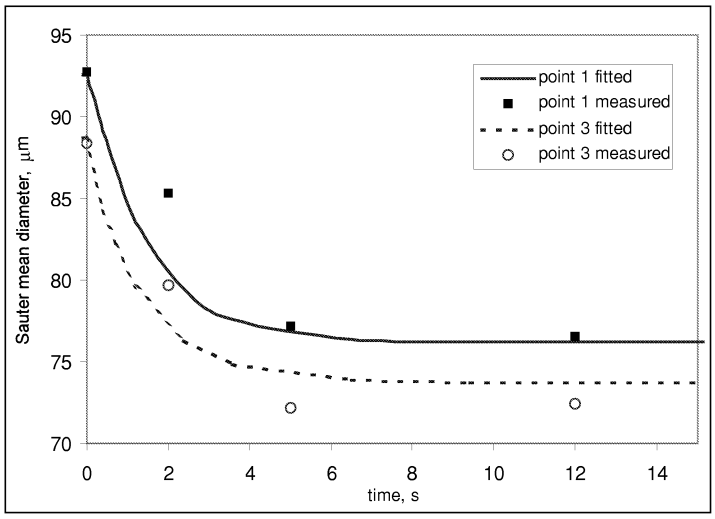

Figure 5. Simulated and measured Sauter mean diameters in the multiblock model during a transient.

The inhomogeneity in the vessel was from 4 to 6 % in the Sauter mean diameter. The calculated drop size distributions are shown in Figure 6. Even though the inhomogeneity was quite small due to a small scale stirred tank, it was enough to be used as a source of data in the parameter estimation.

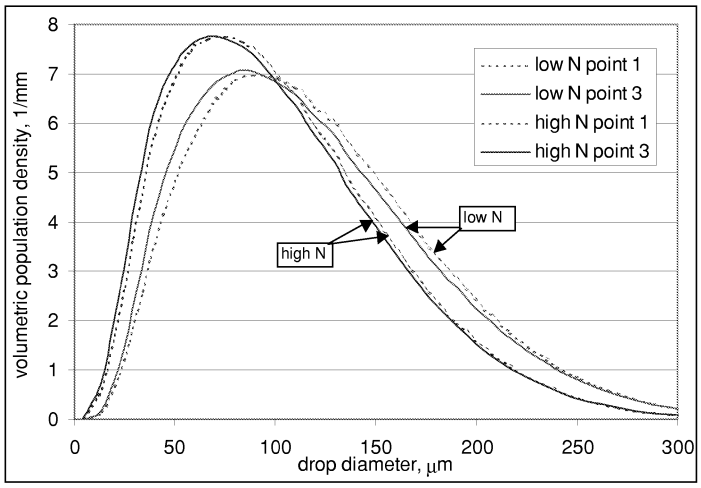

Figure 6. Simulated population densities at two locations of the vessel with two impeller speeds.

5 CONCLUSIONS

Mass transfer models are often important when modeling unit operations and reactors. Accurate calculation of the mass transfer rates is essential when predicting the operation of processes relevant to chemical engineering.

In this work, mass transfer modeling with the Maxwell-Stefan diffusion model was studied. Rigorous modeling of multicomponent mass transfer results in matrix equations and several matrix function calculations. This is very time consuming, especially since these models need to be calculated many times during the solution of a unit operation or reactor model. Some computational simplifications were presented in order to ease the computational work associated with these models. The first was a method to calculate approximately the matrix functions appearing in the multicomponent mass transfer models. The second was a linearization of the high flux correction. Both these methods result in negligible approximation errors in almost all the practical cases. The applicability of these two approximations, along with other modeling aspects, was considered with a distillation tray model. An approximation was also presented in this work for calculating diffusion, and further the mass transfer coefficients, within spherical particles.

The mass transfer rates appearing in the material balances of unit operation or reactor models are products of the mass transfer fluxes and the mass transfer area. Hence, accurate prediction of the mass transfer area is also an important part of the mass transfer modeling. The most fundamental way to calculate the mass transfer area is to use the population balances. However, in many cases the parameters affecting the mass transfer area vary between various parts of the considered balance region. A flow model needs then to be used along with the population balances. One such model is presented in this work, where a stirred tank is divided in a number of subregions describing various turbulence levels in the tank. The drop breakage and coalescence rate parameters of liquid-liquid dispersions are then estimated with experimental data to test the population balance models with the flow model, with a reasonable success. This proves that a flow model can and should be used with the population balances whenever the mass transfer area needs to be calculated accurately.

REFERENCES

1. Alopaeus, V., Aittamaa, J., Nordén, H. V., Approximate High Flux Corrections for Multicomponent Mass Transfer Models and Some Explicit Methods, *Chem. Eng. Sci.* Vol. 54 (1999), pp. 4267-4271.

2. Alopaeus, V., Nordén, H. V., A Calculation Method for Multicomponent Mass Transfer Coefficient Correlations, *Computers & Chem. Eng.* Vol. 23 (1999), pp. 1177-1182.

3. Alopaeus, V., Koskinen, J., Keskinen, K. I., Simulation of the Population Balances for Liquid-Liquid Systems in a Nonideal Stirred Tank, Part 1 Description and Qualitative Validation of the Model, *Chem. Eng. Sci.* Vol. 54 (1999), pp. 5887-5899.

4. Alopaeus, V., Aittamaa, J., Appropriate simplifications in calculation of mass transfer in a multicomponent rate-based distillation tray model, *Ind. Eng. Chem. Res.* Vol. 39 (2000), pp. 4336-4345.

5. Alopaeus, V., Mass Transfer Calculation Methods for Transient Diffusion Within Particles, *AIChE J.* **46** (2000) pp. 2369-2372.

6. Alopaeus, V., Keskinen, K. I., Koskinen, J., Utilization of Population Balances in Simulation of Liquid-Liquid Systems in Mixed Tanks, Presentation at AIChE Annual meeting 2000, Los Angeles, USA

7. Bird, R. B., Stewart, W. E., Lightfoot, E. N., *Transport Phenomena*; Wiley, New York, 1960.

8. Taylor, R., Krishna, R., *Multicomponent Mass Transfer*; Wiley: New York, 1993.

9. Toor, H. L., Solution of the Linearized Equations of Multicomponent Mass Transfer, *AIChE J.* Vol. 10 (1964), pp.460-465.

10. Stewart, W. E., Prober, R., Matrix Calculation of Multicomponent Mass Transfer in Isothermal Systems, *Ind & Eng Chem. Fundam.* Vol. 3 (1964), pp. 224-235.

11. Smith, L., Taylor, R., Film Models for Multicomponent Mass Transfer: A Statistical Comparison, *Ind. Eng. Chem. Fundam.* Vol. 22 (1983), pp. 97-104.

12. Young, T. C., Stewart, W. E., Comparison of Matrix Approximations for Multicomponent Transfer Calculations, *Ind. Eng. Chem. Fundam.* Vol. 25 (1986), pp.476-482.

13. Westerberg, A. W., Hutchison, H. P., Motard, R. L., Winter, P., *Process flowsheeting*, Cambridge University Press, Cambridge, 1979.

14. Krishna, R., Standart, G. L., A Multicomponent Film Model Incorporating a General Matrix Method of Solution to the Maxwell-Stefan Equations, *AIChE J.* Vol. 22 (1976), No 2, pp. 383-389.

15. Haase, R., *Thermodynamics of Irreversible Processes*, Addison-Wesley (1969).

16. Taylor, R., Solution of the Linearized Equations of Multicomponent Mass Transfer, *Ind. Eng. Chem. Fundam.* Vol. 21 (1982), pp. 407-413.

17. Valentas, K. J., Amundson, N. R., Breakage and Coalescence in Dispersed Phase Systems, *Ind. Eng. Chem. Fundam.* Vol. 5 (1966), pp. 533-542.

18. Hsia, M. A., Tavlarides, L. L., A Simulation Model for Homogeneous Dispersion in Stirred Tanks, *Chem. Eng. J.* Vol. 20 (1980), pp. 225-236.

19. Tadayyon, A., Rohani, S., Determination of Particle Size Distribution by Par-Tec® 100: Modeling and Experimental Results, *Part. Part. Syst. Charact.* Vol. 15 (1998), pp. 127-135.

20. Narsimhan, G., Gupta, J. P., Ramkrishna, D., A Model for Transitional Breakage Probability of Droplets in Agitated Lean Liquid-Liquid Dispersions, *Chem. Eng. Sci.* Vol. 34 (1979), pp. 257-265.

21. Coulaloglou, C. A., Tavlarides, L. L., Description of Interaction Processes in Agitated Liquid-Liquid Dispersions, *Chem. Eng. Sci*. Vol. 32 (1977), pp. 1289-1297.

22. Tsouris, C., Tavlarides, L. L., Breakage and Coalescence Models for Drops in Turbulent Dispersions, *AIChE J*. Vol. 40 (1994), pp. 395-406.

23. Bapat, P. M., Tavlarides, L. L., Smith, G. W., Monte Carlo Simulation of Mass Transfer in Liquid-Liquid Dispersions, *Chem. Eng. Sci.* Vol. 38 (1983), pp. 2003-2013

APPENDICES